ICTMC-16に向けた研究討論会
2008.8.22

Characterization of Fe 3d states in $CuFeS_2$ by X-ray emission spectroscopy

K. Sato[1,2], Y. Harada[3], M. Taguchi[3], S. Shin[3] and A. Fujimori[4]

1. Tokyo University of Agriculture and Technology
2. Japan Science and Technology Agency
3. RIKEN/Spring-8
4. University of Tokyo

CONTENTS

- Introduction: Review on experimental studies on the 3d electronic states of Fe in chalcopyrite $CuFeS_2$ and $CuAlS_2$:Fe
- Overview of X-ray Emission Spectroscopy Why and how XES provides information on d-d transitions buried in the CT absorption
- XES of $CuFeS_2$
- Interpretation of XES results

Introduction

- In the following is presented a review on experimental and theoretical studies on the 3d electronic states of Fe in chalcopyrite $CuFeS_2$, $CuGaS_2$:Fe and $CuAlS_2$:Fe

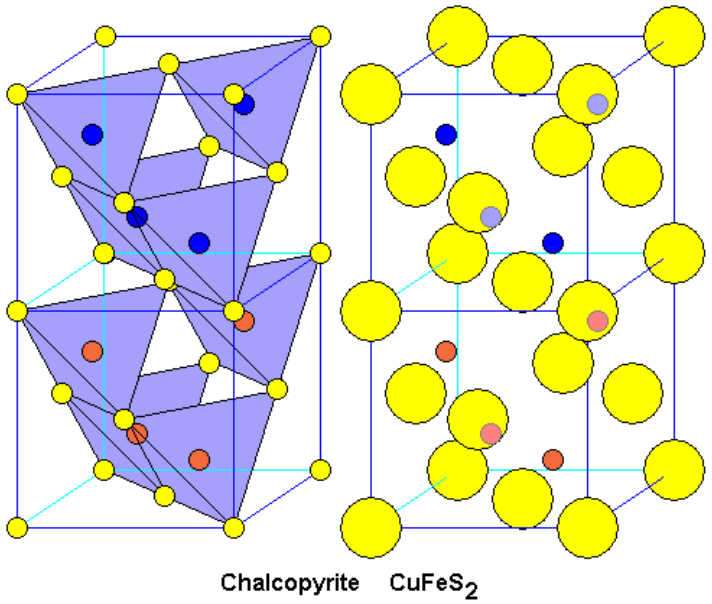

http://www.uwgb.edu/dutchs/PETROLGY/Sphal-Chalc%20Structure.HTM

Cu

Fe

S

Cells with iron atoms (orange) alternate with cells containing copper (blue).

www.asahi-net.or.jp/~ug7s-ktu/e_odo.htm

Mystery of $CuFeS_2$

- Chalcopyrite, $CuFeS_2$ is a mineral compound with a golden lustre and has been known as a semiconductor with an antiferromagnetic ordering. The local magnetic moment of Fe has been known to be as small as 3.85 μ_B from neutron scattering experiments[1].
- The result is conflicting with ionic bonding model of $CuFeS_2$ in which high spin $Fe^{3+}(3d^5)$ with local moment of 5 μ_B is expected.
- To elucidate the electronic structure of $CuFeS_2$ optical studies has been conducted in single crystals of $CuGaS_2$:Fe and $CuAlS_2$:Fe as well as $CuFeS_2$.

[1] G.Donnay, L.M. Corliss, J.D.H. Donnay, N. Elliot and J.M. Hastings: Symmetry of Magnetic Structures: Magnetic Structure of Chalcopyrite Phys. Rev. 112 (1958) 1917-1923.

Optical absorption spectrum in $CuFeS_2$ and $CuGaS_2$:Fe and $CuAlS_2$:Fe

- In order to elucidate electronic structures of Fe in $CuFeS_2$, Teranishi and Sato studied optical spectroscopy in Fe-doped chalcopyrite-type semiconductors, $CuAlS_2$ and $CuGaS_2$, and found broad and strong absorption band with two peaks around 1.3 eV and 1.9 eV [2]

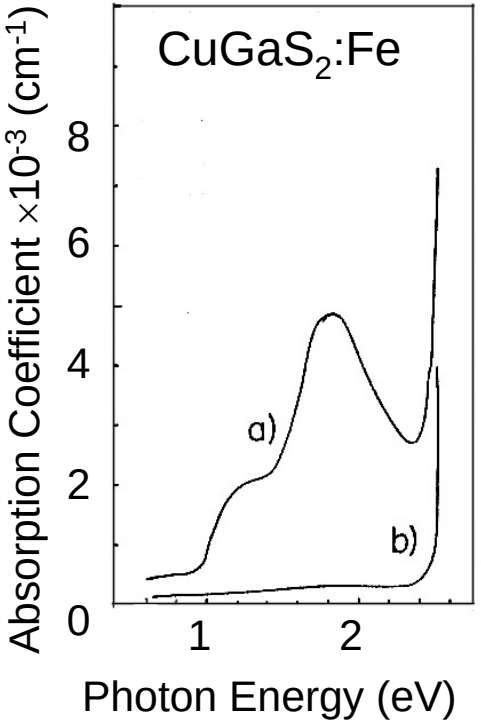

a) $CuGaS_2$:$Fe_{0.006}$, b) $CuGaS_2$

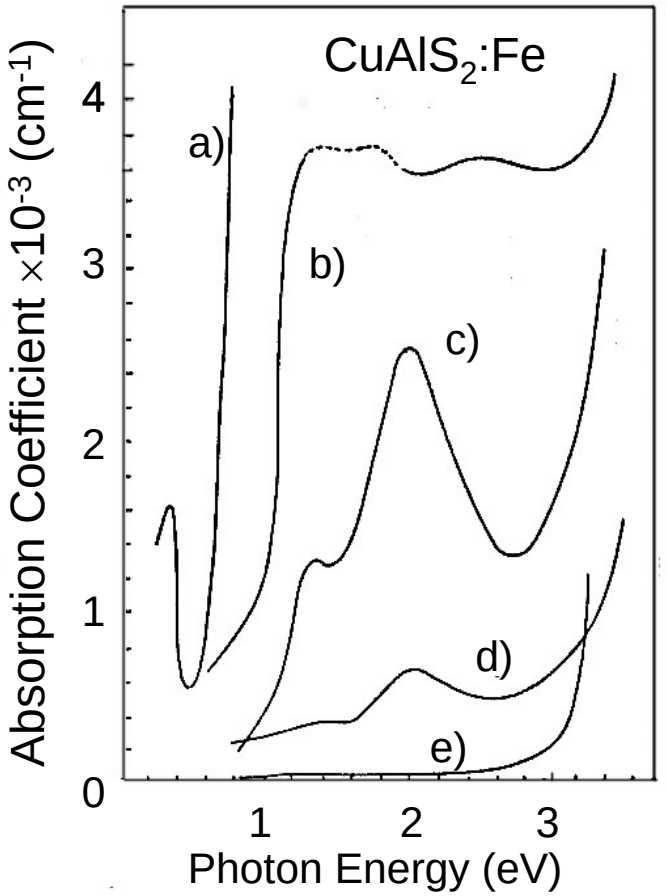

a) $CuFeS_2$, b) $CuAlS_2$:$Fe_{0.07}$, c) $CuAlS_2$:$Fe_{0.006}$, d) $CuAlS_2$:$Fe_{0.0008}$, e) $CuAlS_2$

[2] T. Teranishi and K. Sato: J. Phys. Soc. Jpn. 36 (1974) 1618-1624.

Theoretical Studies on the Energy Band of $CuFeS_2$

- Kambara calculated absorption spectra of $CuFeS_2$ and $CuGaS_2$:Fe using a model cluster consisting of 17 atoms.
- Energy gap between occupied and unoccupied levels is 1.0eV and 1.5eV in CuGaS2:Fe corresponding to observed absorption band energies.
- If antiferromagnetic configuration is assumed Fe moment is $2.8\mu_B$ at the center Fe and $-3.7\mu_B$ at the corner Fe. Overlap of 3d orbitals is responsible to the reduction.

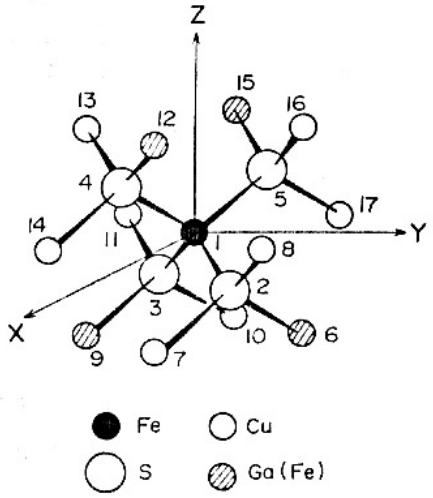

Fig. 1. 17-atom cluster and the coordinate system.

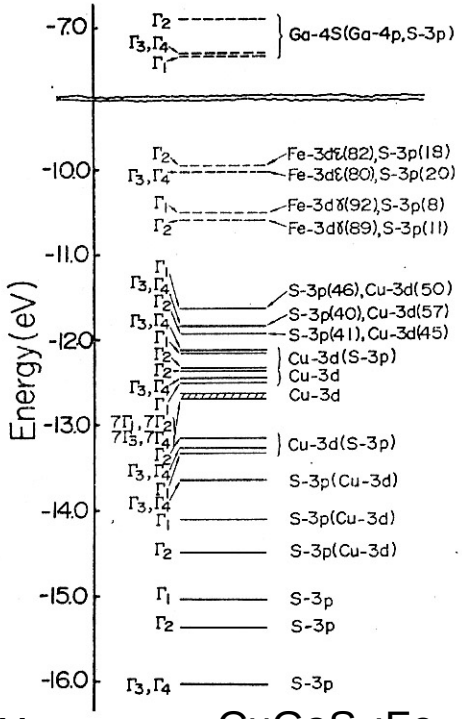

$CuGaS_2$:Fe

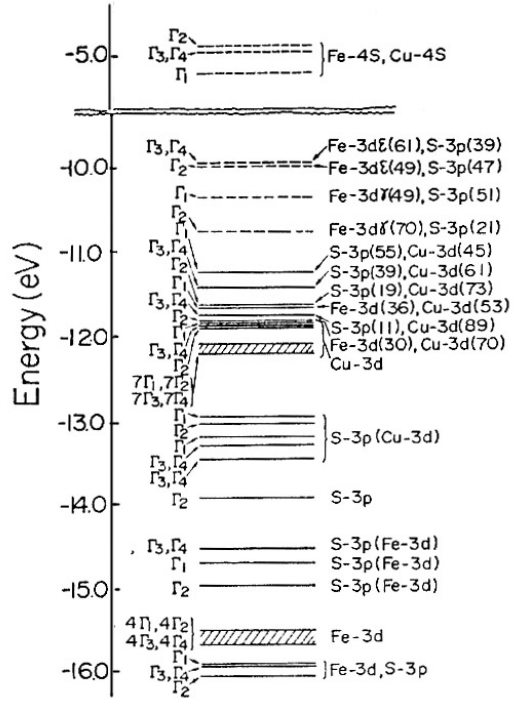

$CuFeS_2$

T. Kambara: J. Phys. Soc. Jpn. 36 (1974) 1625-1634

Infrared photoluminescence spectra in $CuGaS_2$:Fe and $CuAlS_2$:Fe

- Sharp photoluminescence (PL) peak was found around 0.61 eV ($CuGaS_2$) and 0.72 eV ($CuAlS_2$) . A Zeeman spectrum analysis allowed us to assign the sharp PL lines to the ligand-field transition from an excited state $^4T_1$ to a ground state $^6A_1$ in the $3d^5$ manifold of Fe^{3+}.

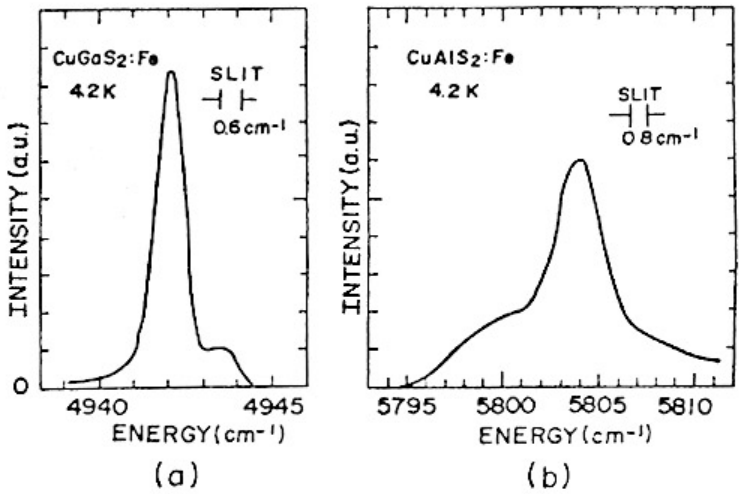

Fig. 1. The luminescence spectra of (a) $CuGaS_2$: Fe and (b) $CuAlS_2$:Fe at 4.2 K.

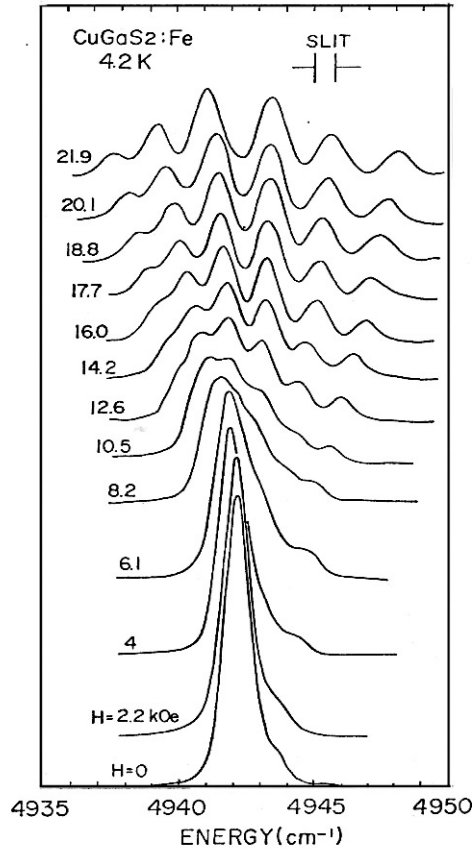

Fig. 4. The Zeeman spectra of the zero line of $CuGaS_2$:Fe at 4.2 K. The spectra are arbitrarily shifted for the sake of clarity.

K.Sato and T.Teranishi: Infrared Luminescence of Fe3+ in CuGaS2 and CuAlS2; J. Phys. Soc. Jpn. 37 [2] (1974) 415-422.

Interpretation of IR luminescence spectrum by Ligand-field theory

- The observed IR PL was interpreted as a ligand field transition from ^4E manifold derived from $^4T_1$ of $3d^5$ state in Fe^{3+}, taking into account the Zeeman spectra of the PL line.
- However, extremely reduced values of the Racah parameters were necessary to account for the enrgy position of the IR PL.

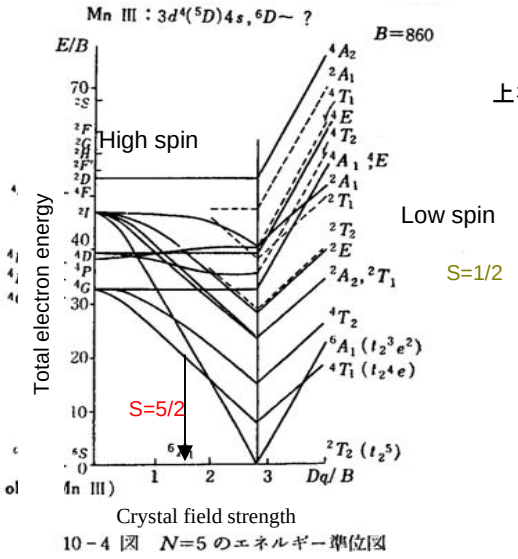

10－4 図 $N=5$ のエネルギー準位図

上村，菅野，田辺「配位子場理論とその応用」(裳華房)

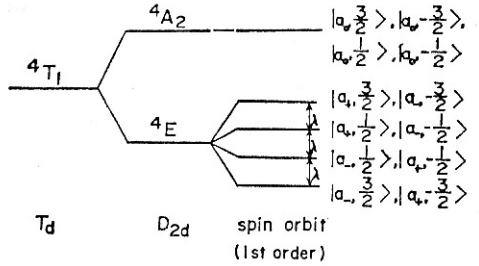

Fig. 7. A proposed energy level scheme for the excited state ($^4T_1$) of Fe^{3+} with a tetragonal distortion (D_{2d}) and a spin-orbit interaction. In this figure $a_\pm = \mp 1/\sqrt{2}(\alpha \pm i\beta)$ and $a_0 = \gamma$.

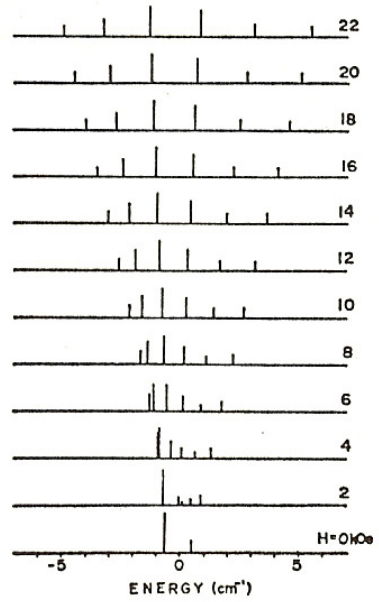

Fig. 8. The predicted Zeeman spectra for various magnitudes of the magnetic field. The excited state is assumed to be represented by $|a_-, +3/2>$ and $|a_+, -3/2>$.

Molecular orbital + CI calculation in the Fe-S4 cluster

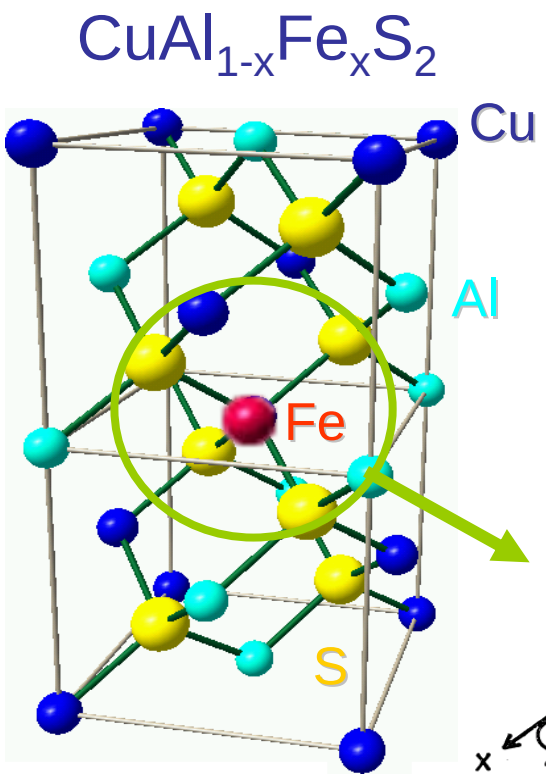

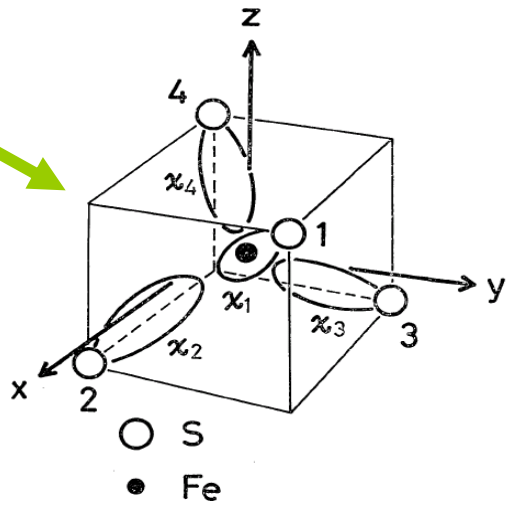

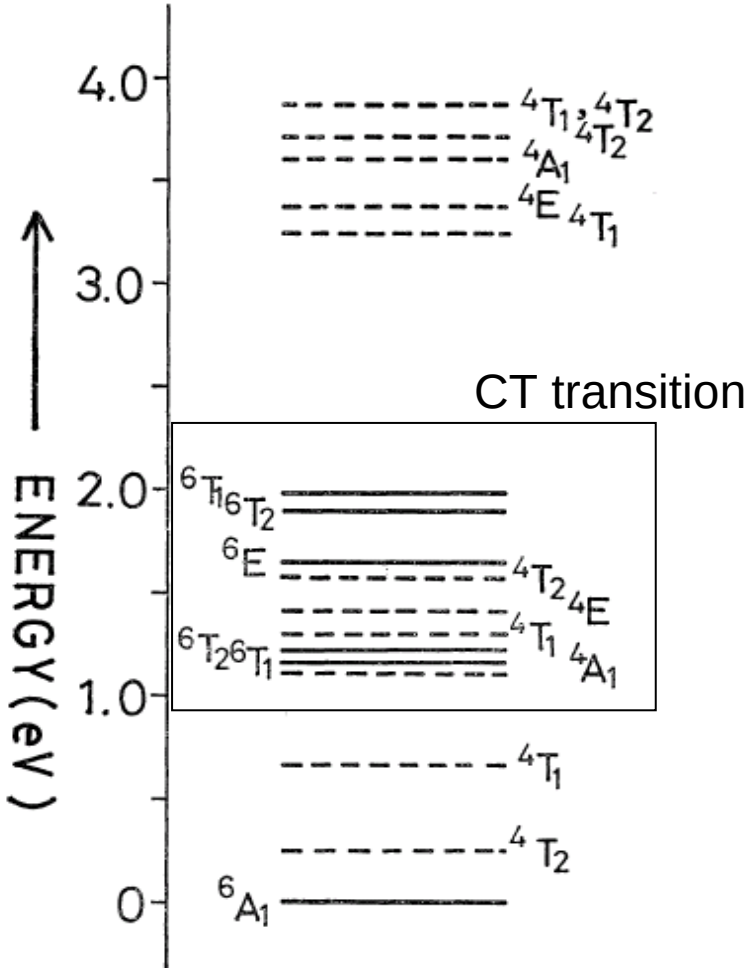

T. Kambara, K. Suzuki and K. Gondaira, Electronic States of Fe in I-III-VI2 Compounds, JPSJ 39 764-771 (1975)

Haldane-Anderson mechanism for the formation of localized "*d*" states in negtive-Δ systems

Δ > 0

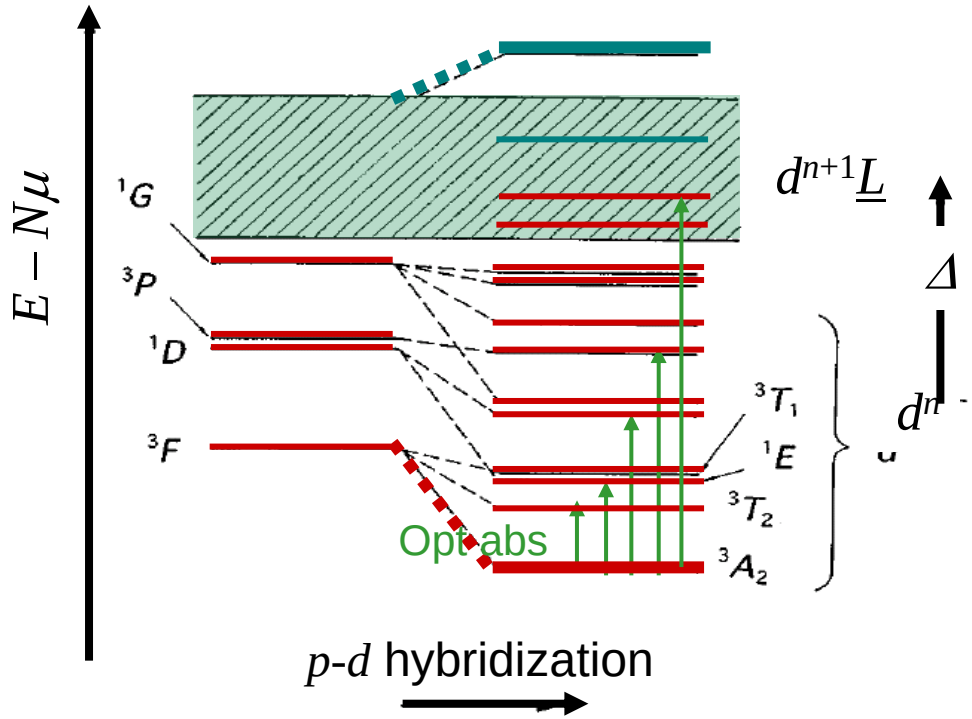

Δ < 0

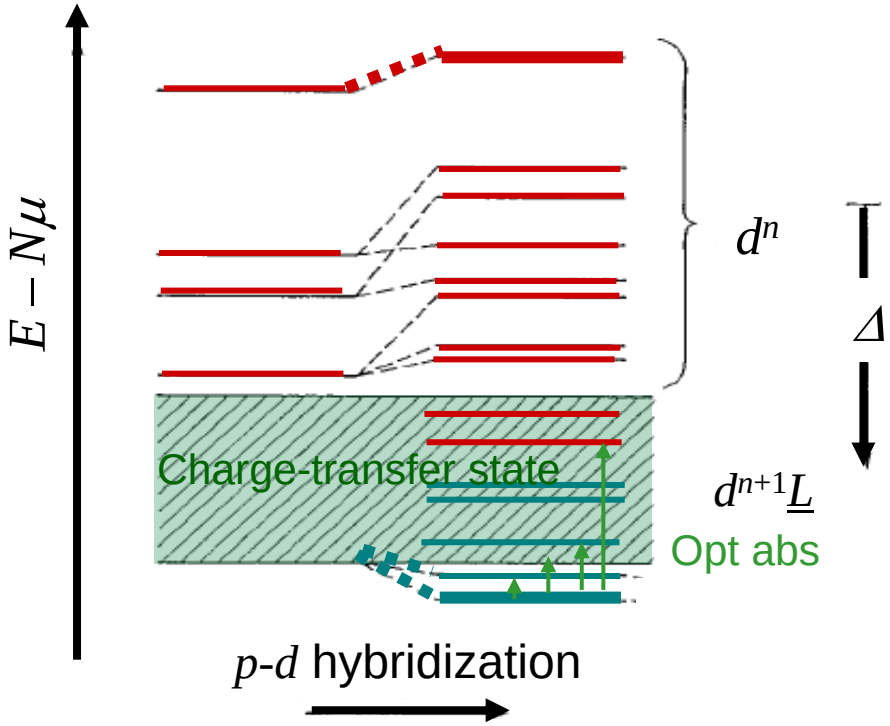

$\Delta = E(d^{n+1}\underline{L}) - E(d^n)$: Charge-transfer energy

M. Imada, A. Fujimori, Y. Tokura, RMP '98

Electronic structure of transition-metal compounds

Mott-Hubbard type insulator

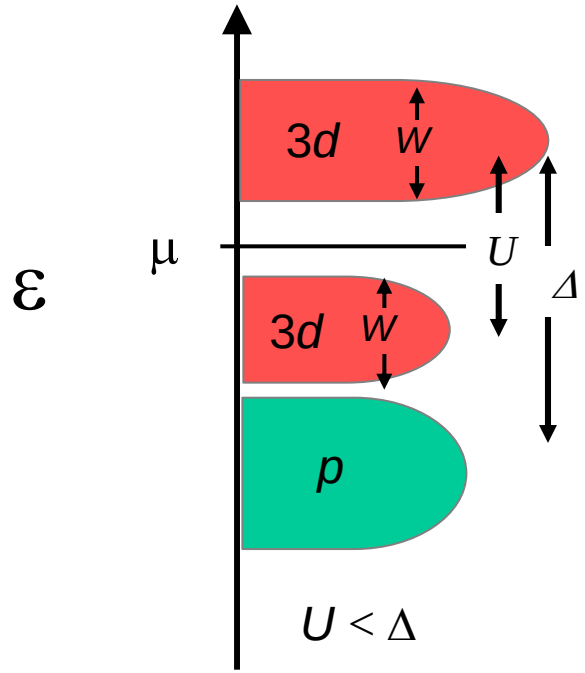

gap ~ U - W

Charge-transfer-type insulator

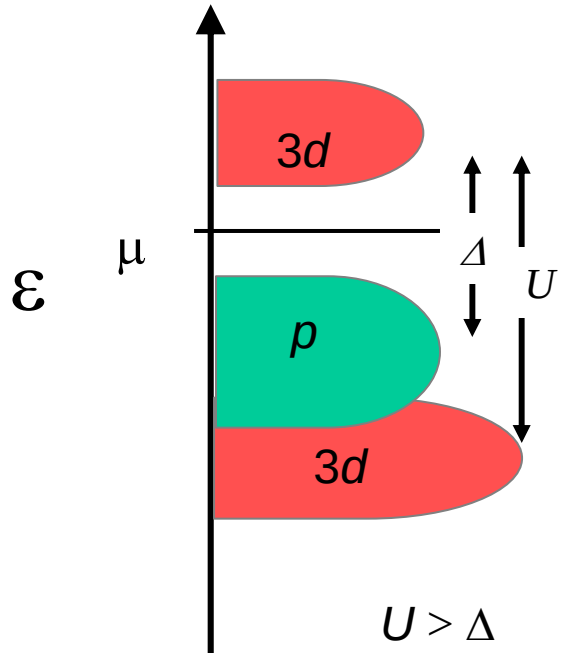

gap ~ Δ - W

W: bandwidth ~3 eV
U : Coulomb energy ~7 eV
Δ: Charge-transfer energy

Chemical trend in charge-transfer energy Δ

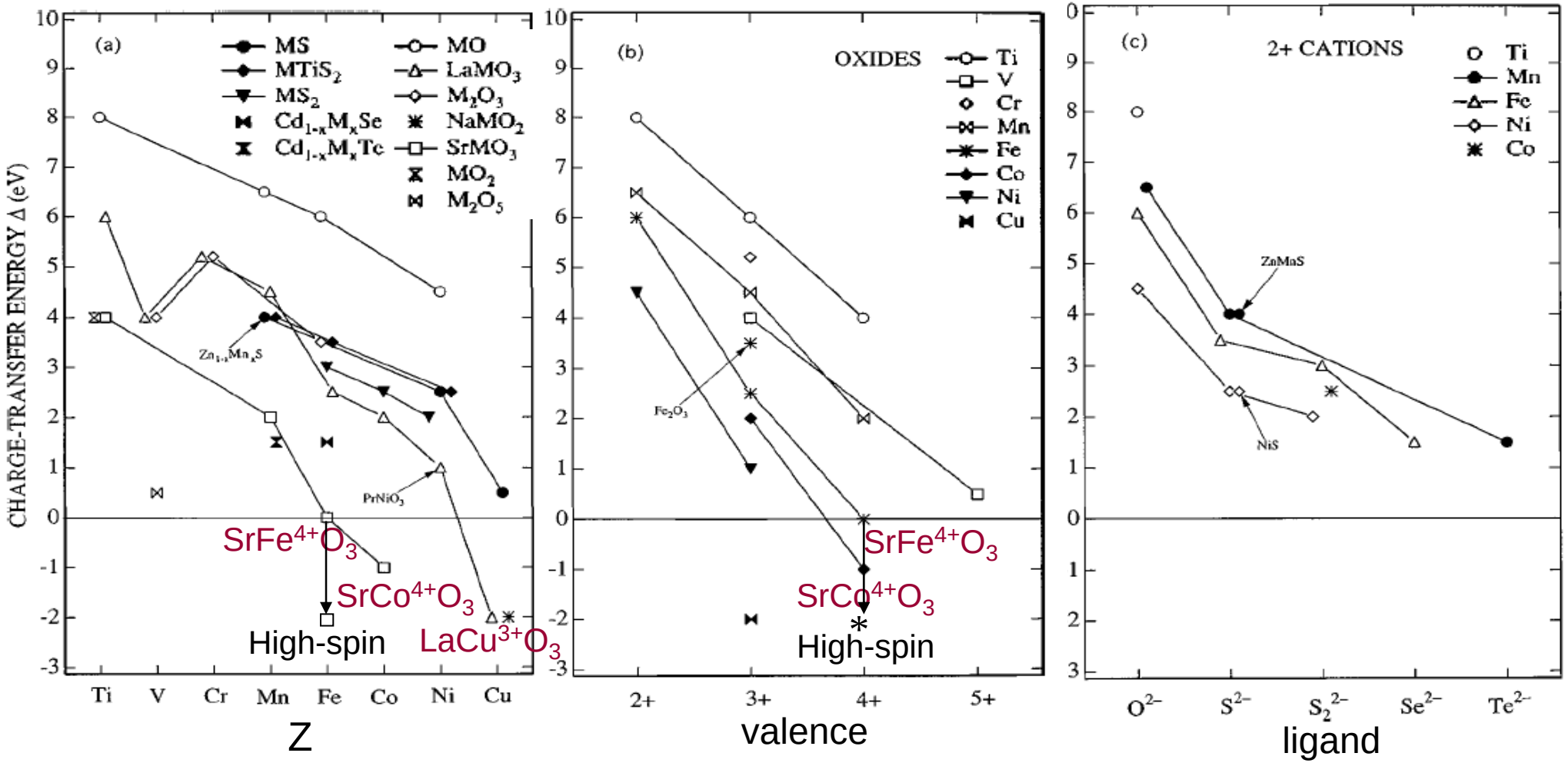

$\Delta = E(d^{n+1}\underline{L}) - E(d^n)$: Charge-transfer energy

A.E. Bocquet et al., PRB '92
M. Imada, A. Fujimori, Y. Tokura, RMP '98

Chemical trend in charge-transfer energy Δ

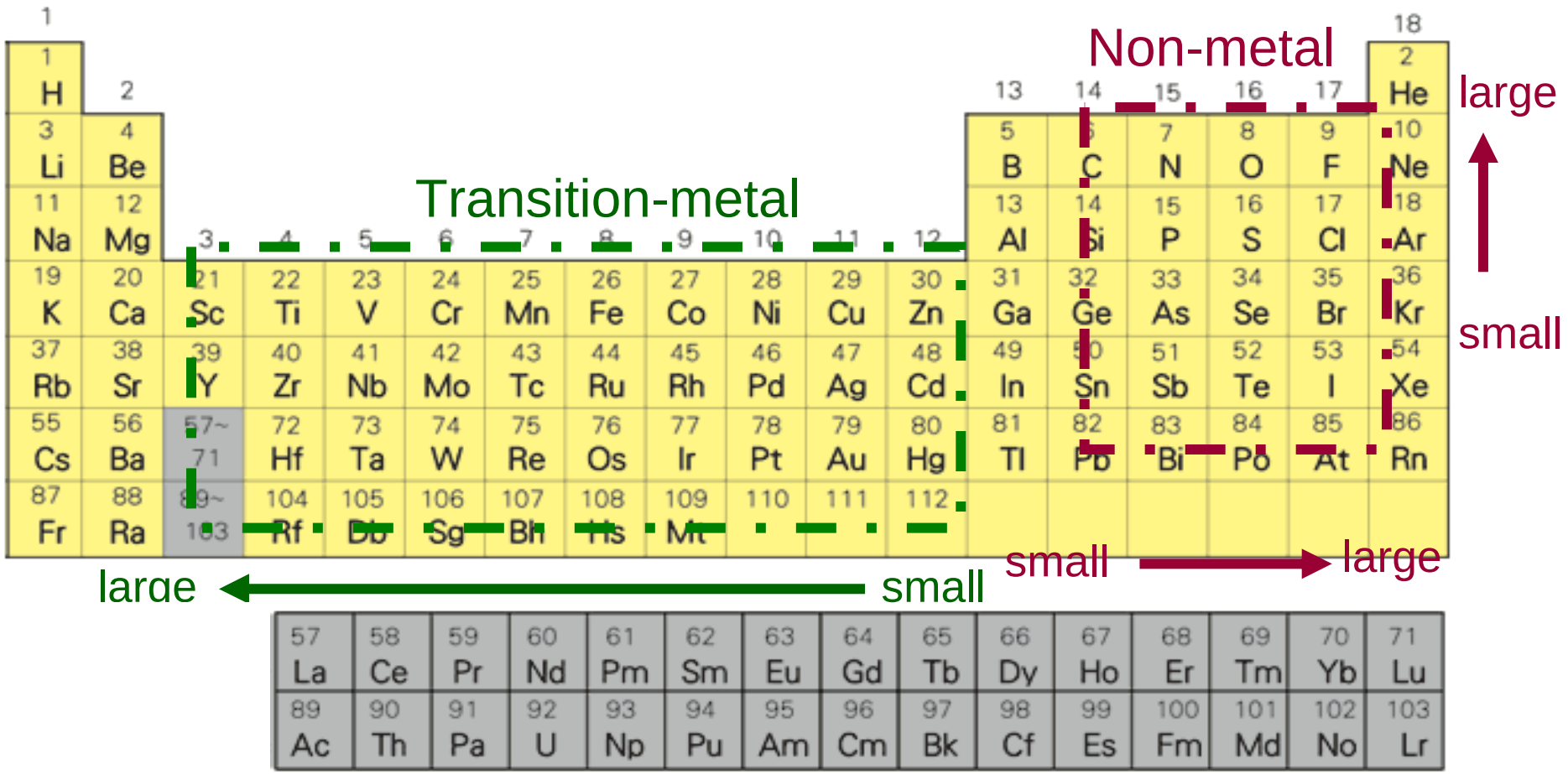

valence : 2- - …. + 2+ 3+ 4+ 5+

large ← small

負の電荷移動エネルギーをもつ磁性半導体カルコパイライト型$CuFeS_2$

価電子帯光電子スペクトル

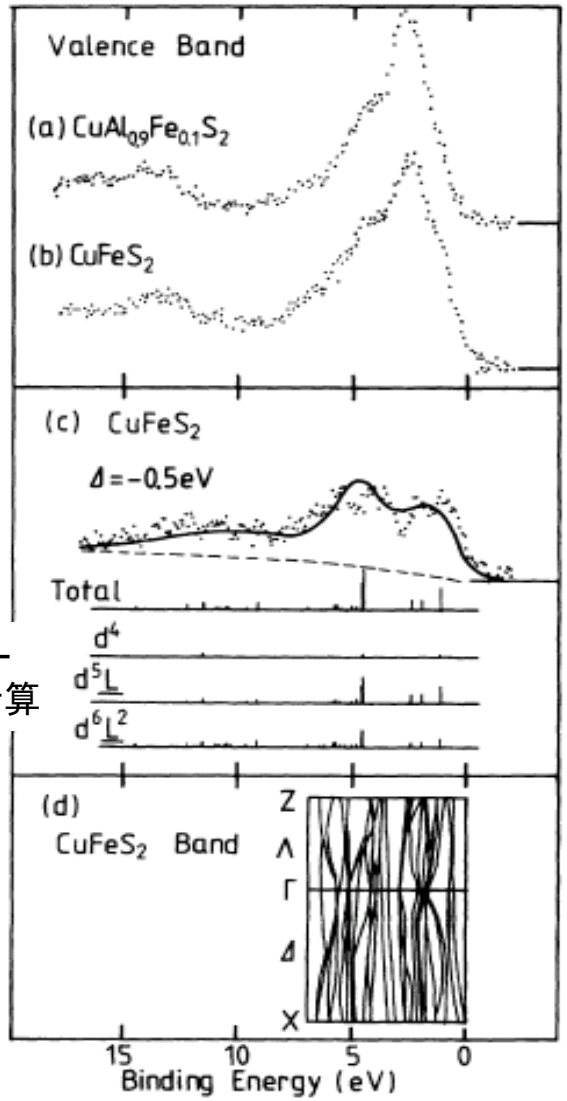

クラスター
モデルCI計算

Fe内殻光電子スペクトル

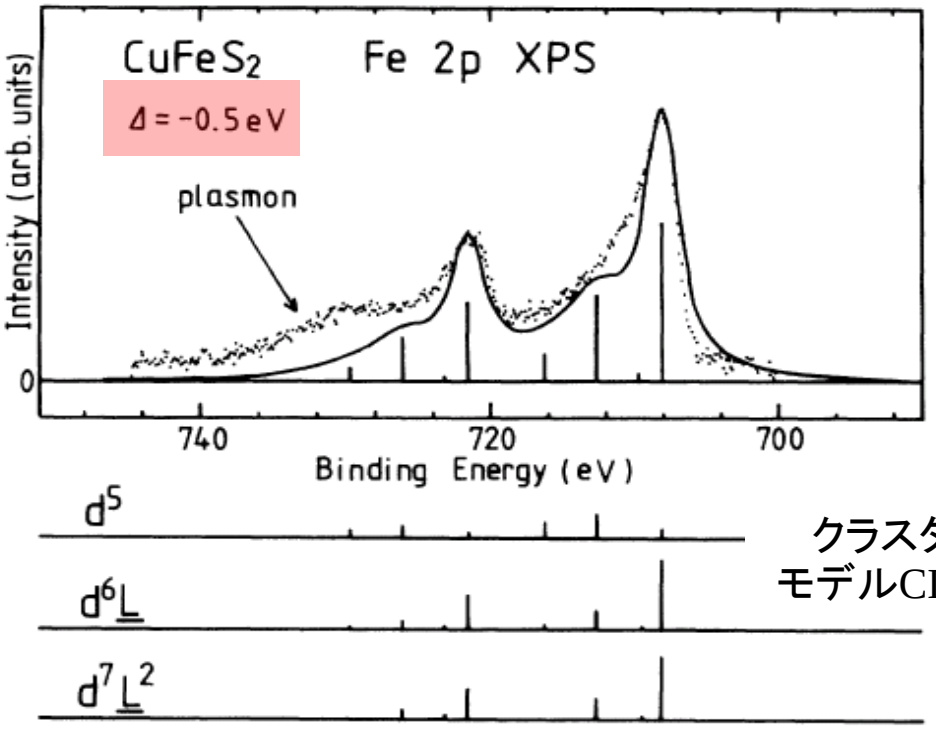

クラスター
モデルCI計算

M.Fujisawa, S.Suga, T.Mizoguchi, A.Fujimori and K.Sato:
Electronic Structures of CuFeS2 and CuAl0.9Fe0.1S2
Studied by Electron and Optical Spectroscopies;
Phys. Rev. B49 [11] (1994) 7155-7164.

Electronic structure of transition-metal compounds

Mott-Hubbard type insulator

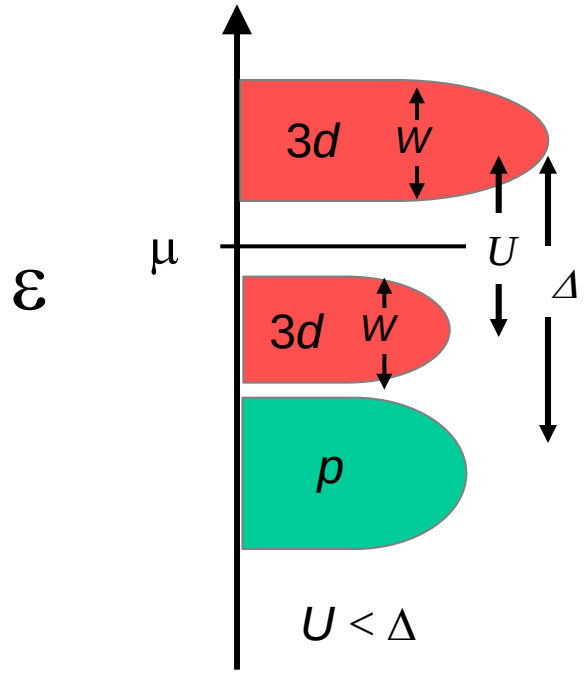

gap ~ U - W

Charge-transfer-type insulator

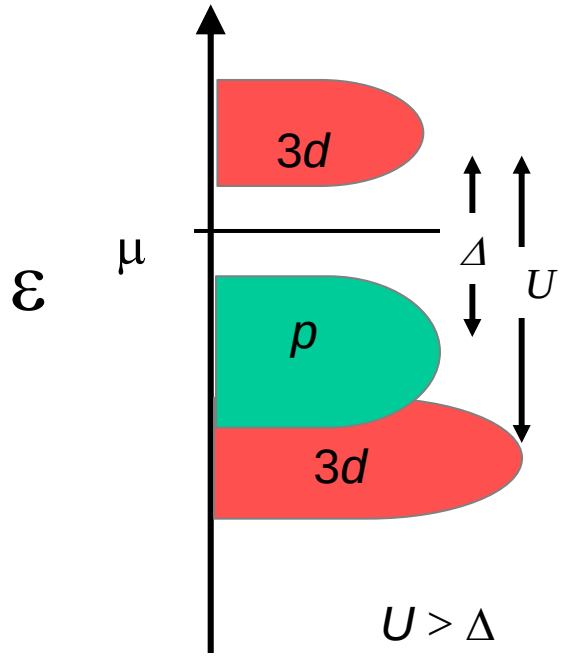

Metal?

Indeed, $SrFeO_3$ is a metal. However, ….

gap ~ Δ - W

W: bandwidth ~3 eV
U : Coulomb energy ~7 eV
Δ: Charge-transfer energy

Haldane-Anderson mechanism for the formation of localized "*d*" states in negtive-Δ systems

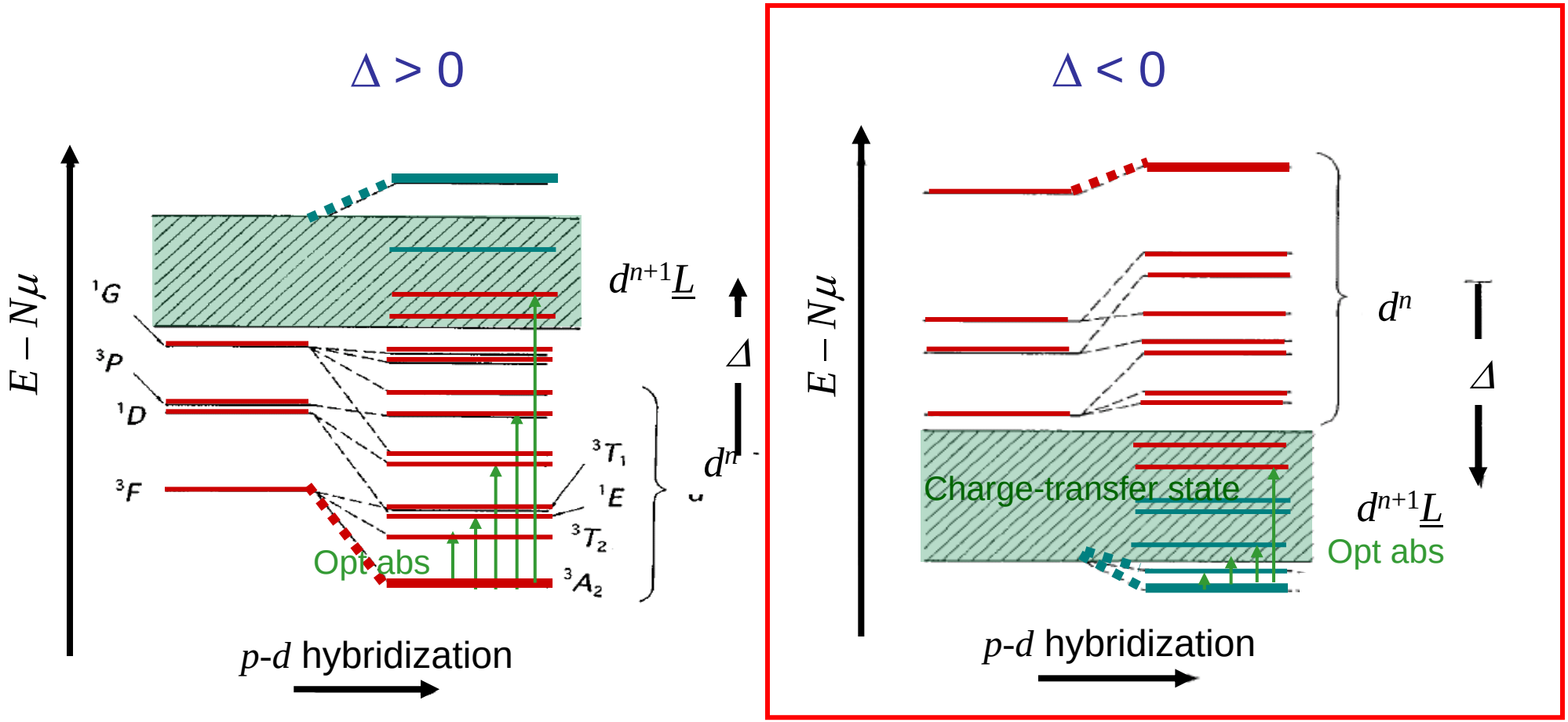

$\Delta = E(d^{n+1}\underline{L}) - E(d^n)$: Charge-transfer energy

M. Imada, A. Fujimori, Y. Tokura, RMP '98

Chemical trend in charge-transfer energy Δ

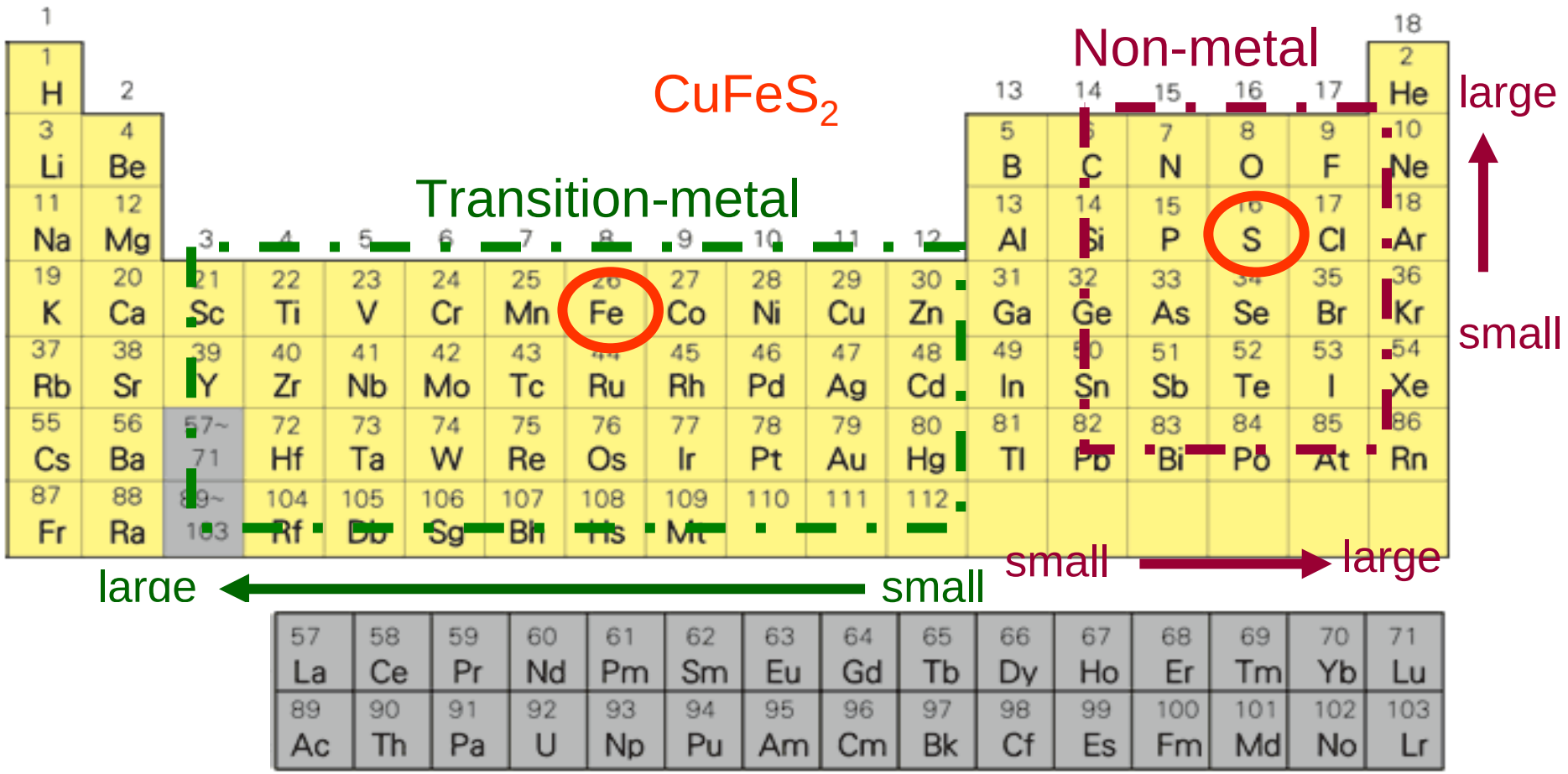

valence : 2- - …. + 2+ 3+ 4+ 5+

large ← small

Zaanen-Sawatzky-Allen相図

なぜ絶縁体なのか？

模式図

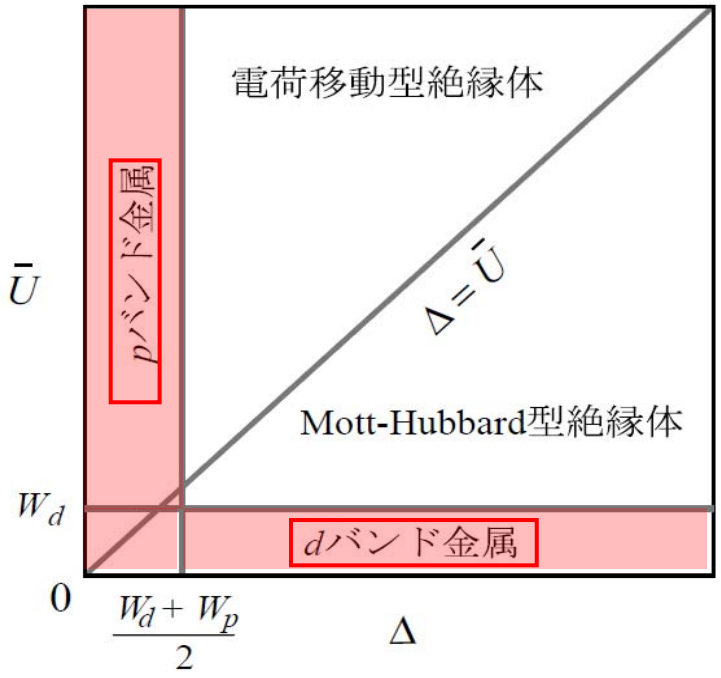

実際の物質

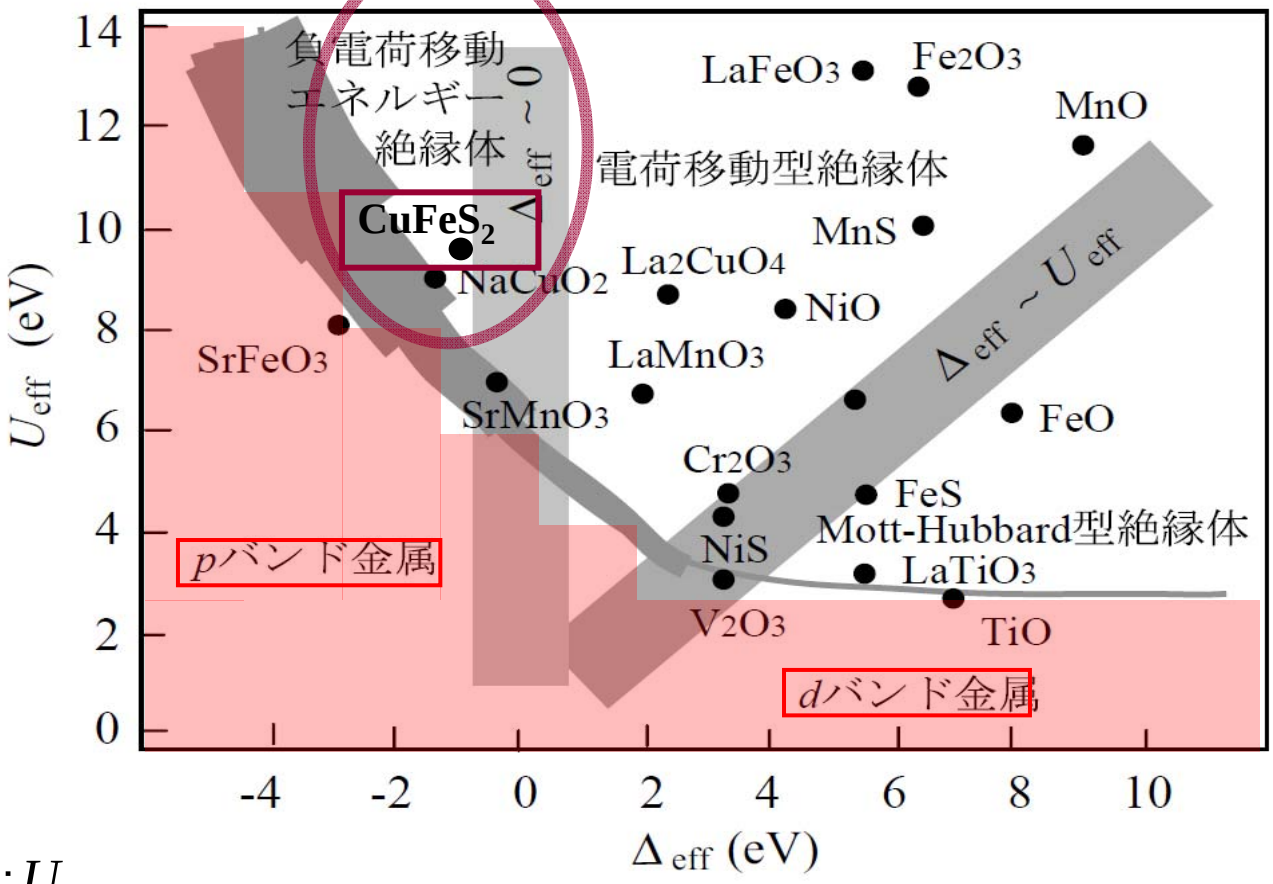

電荷移動エネルギー：Δ
原子内クーロンエネルギー：U

Unusually low-energy *d-d* optical absorption peak

Optical absorption due to $Fe^{3+}(d^5)$ ion in chalcopyrite-type I-III-VI2 semiconductor

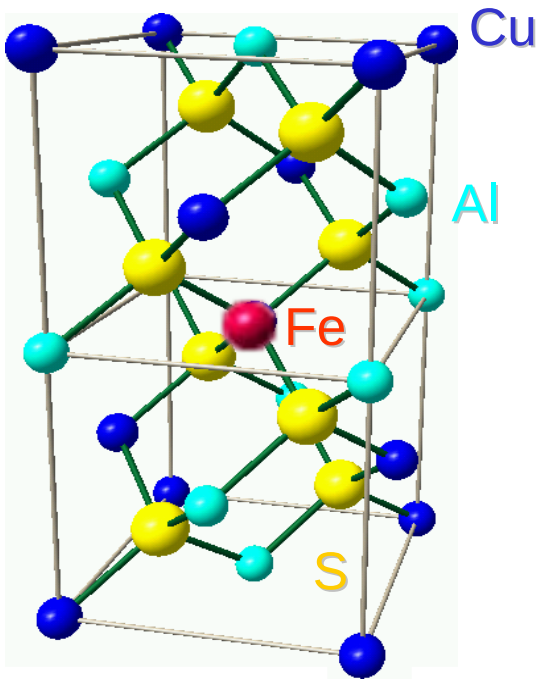

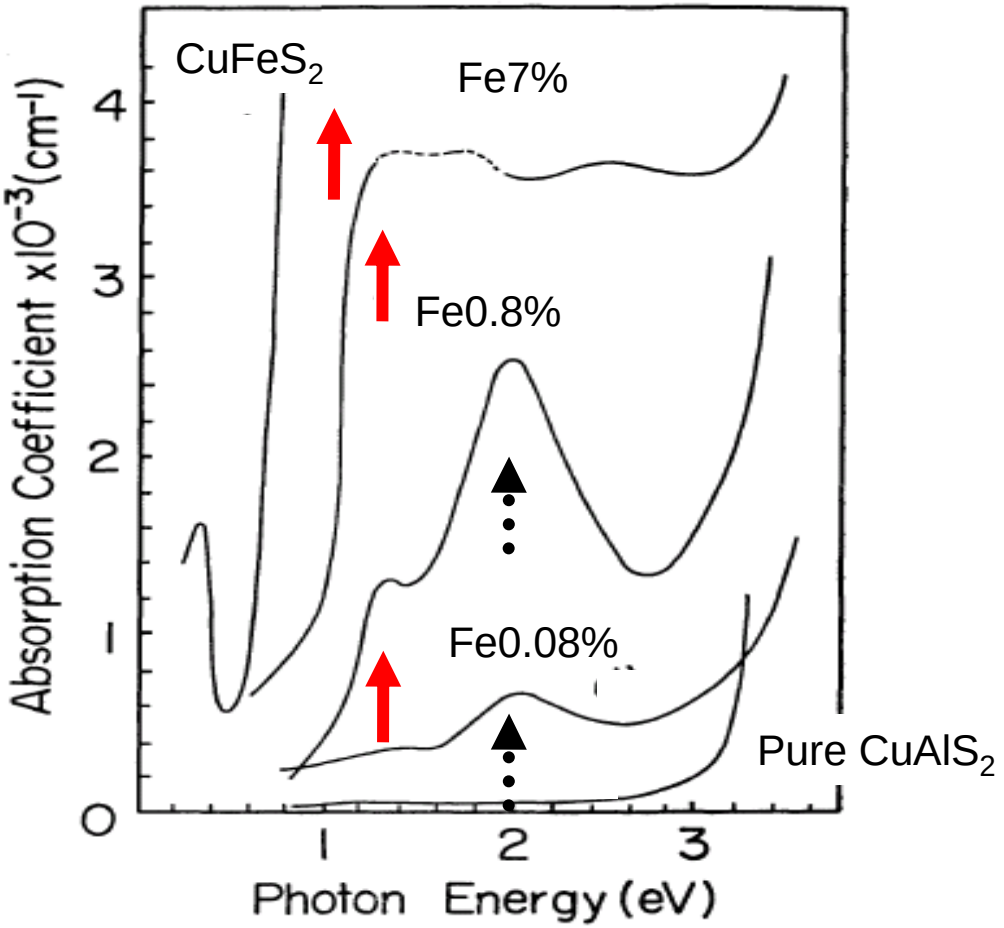

T. Teranishi and K. Sato, J. Phys. Soc. Jpn. ’74

電荷移動励起に隠れたd-d遷移を見る
―共鳴非弾性X線散乱（RIXS）―

Resonant inelastic x-ray scattering（RIXS)

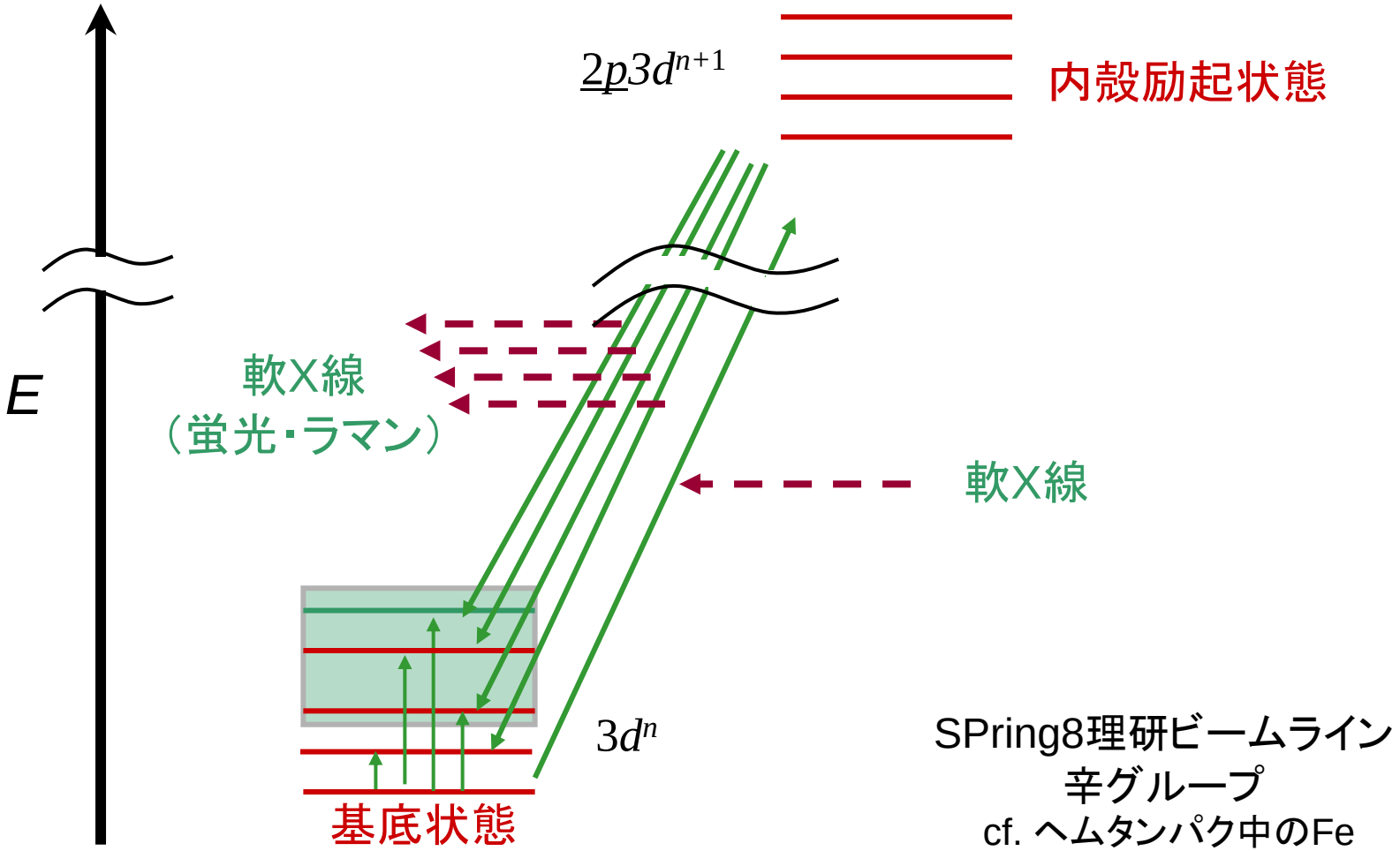

SPring8理研ビームライン
辛グループ
cf. ヘムタンパク中のFe

XAS & XES

X-ray absorption(XAS) and emission(XES) spectroscopy

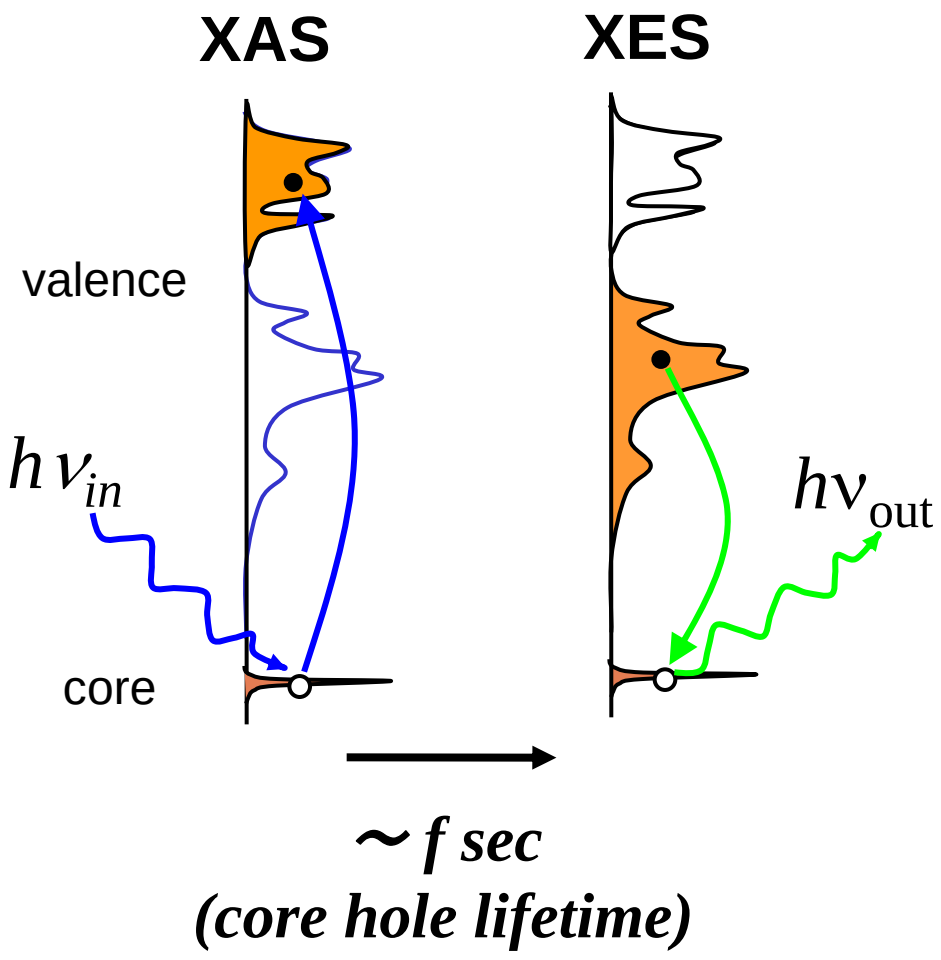

- XAS probes unoccupied electronic states
- XES probes occupied electronic states

- Applicable to solids ranging from metals to wide gap insulators
- Large probing depth
- Element specificity

SPring-8 BL27SU c3 station

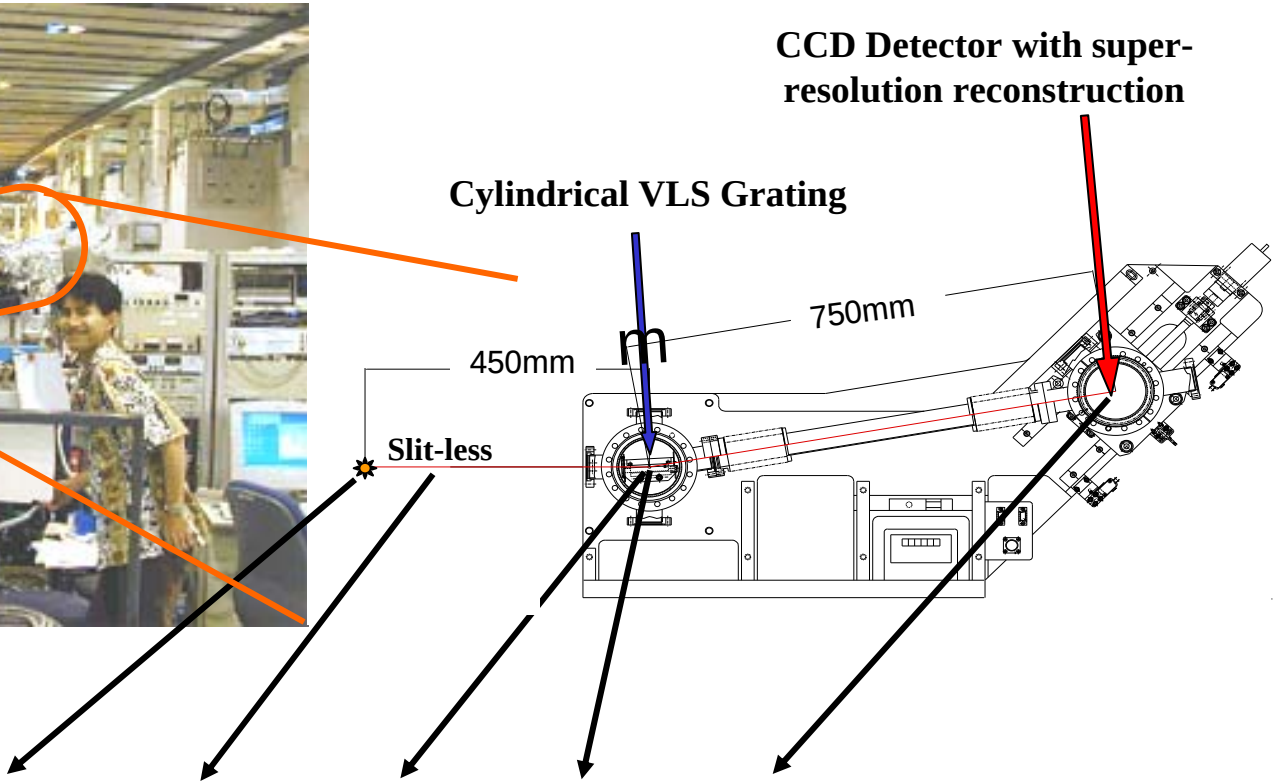

	Mount type	Spot size (μm)	Slit width (μm)	Lines/mm & α (deg.)	Radius (mm)	Detector type	Resolution(eV) @ Fe 2*p* edge
BL27SU	Flat Field type	7~10	None	Valid line 2200 & 87.5	8940	背面照射型 CCD(2k x 2k)	0.6

T. Tokushima Y. Harada, H. Ohashi, Y. Senba, S. Shin, Rev.Sci.Instruments 77 (2006) 063107

Polarization dependence

depolarized and polarized configurations for the XES measurement

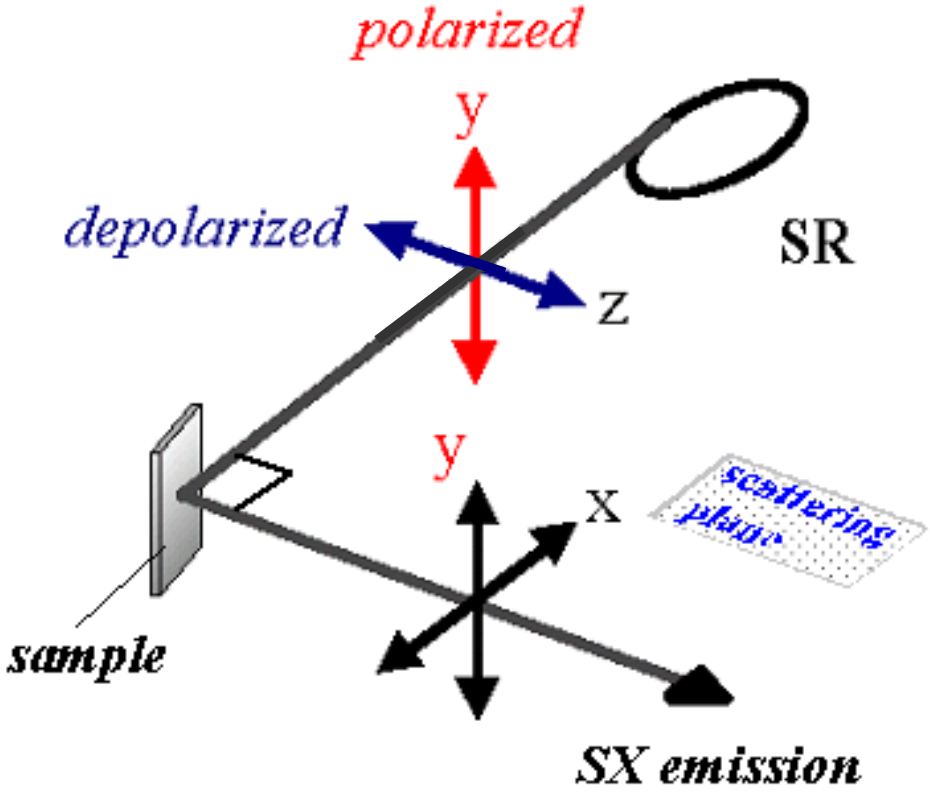

'depolarized' configuration
polarization vector of the incident photon is NOT included in detected photons

'polarized' configuration
polarization vector of the incident photon is included in detected photons

Experimental results (XAS)

XAS experiment : Y. Mikhlin et al., J. Electron Spectrosc. Relat. Phenom. **142**,83 (2005)

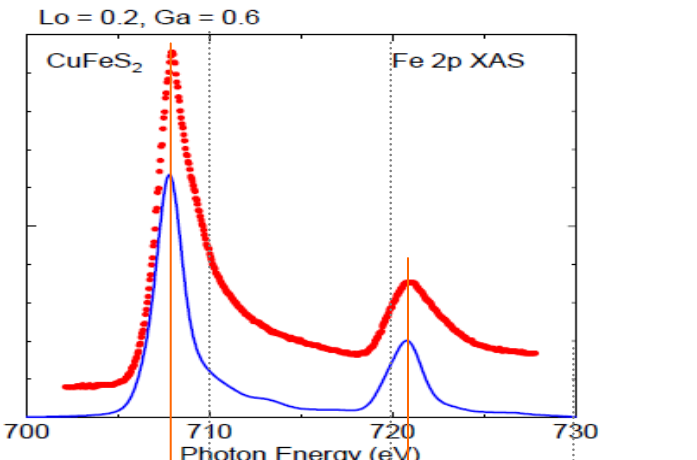

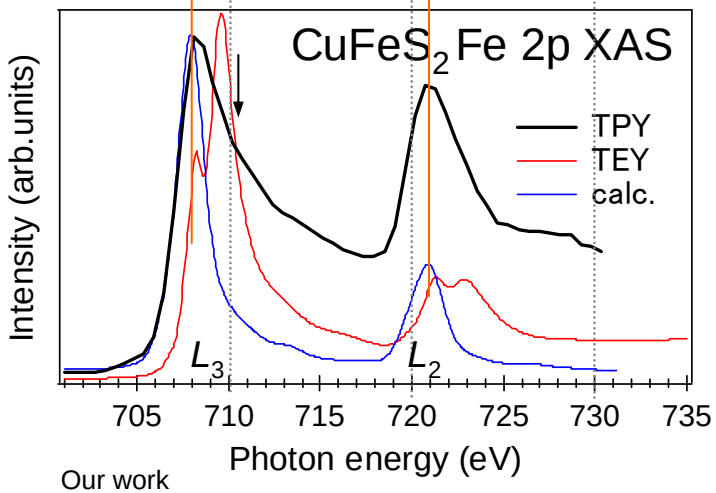

Our work

or

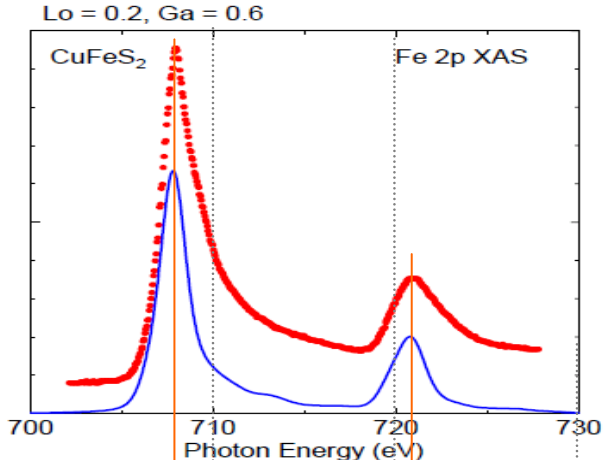

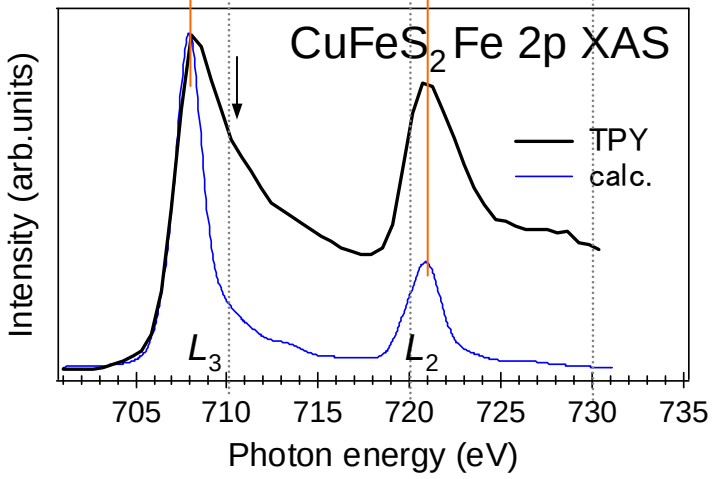

Transition Metal *L*-edge RIXS

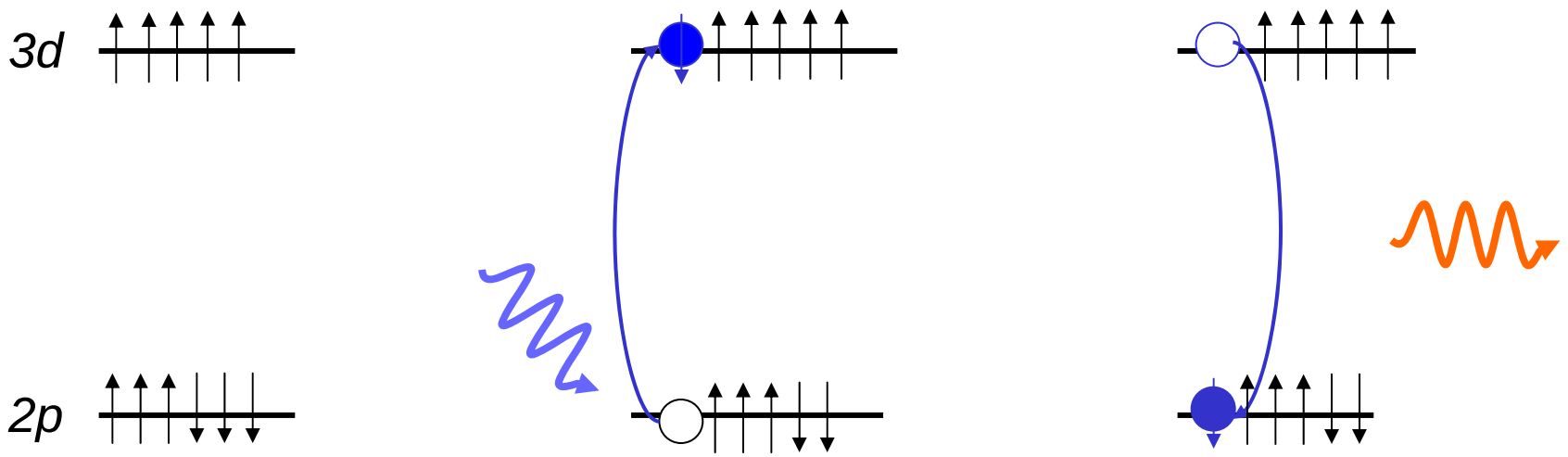

Initial state

$|3d^n\rangle$

Intermediate state

$|2p^5\,3d^{n+1}\rangle$

Final state

$|3d^n\rangle$

dd excitation ($3d^5$)

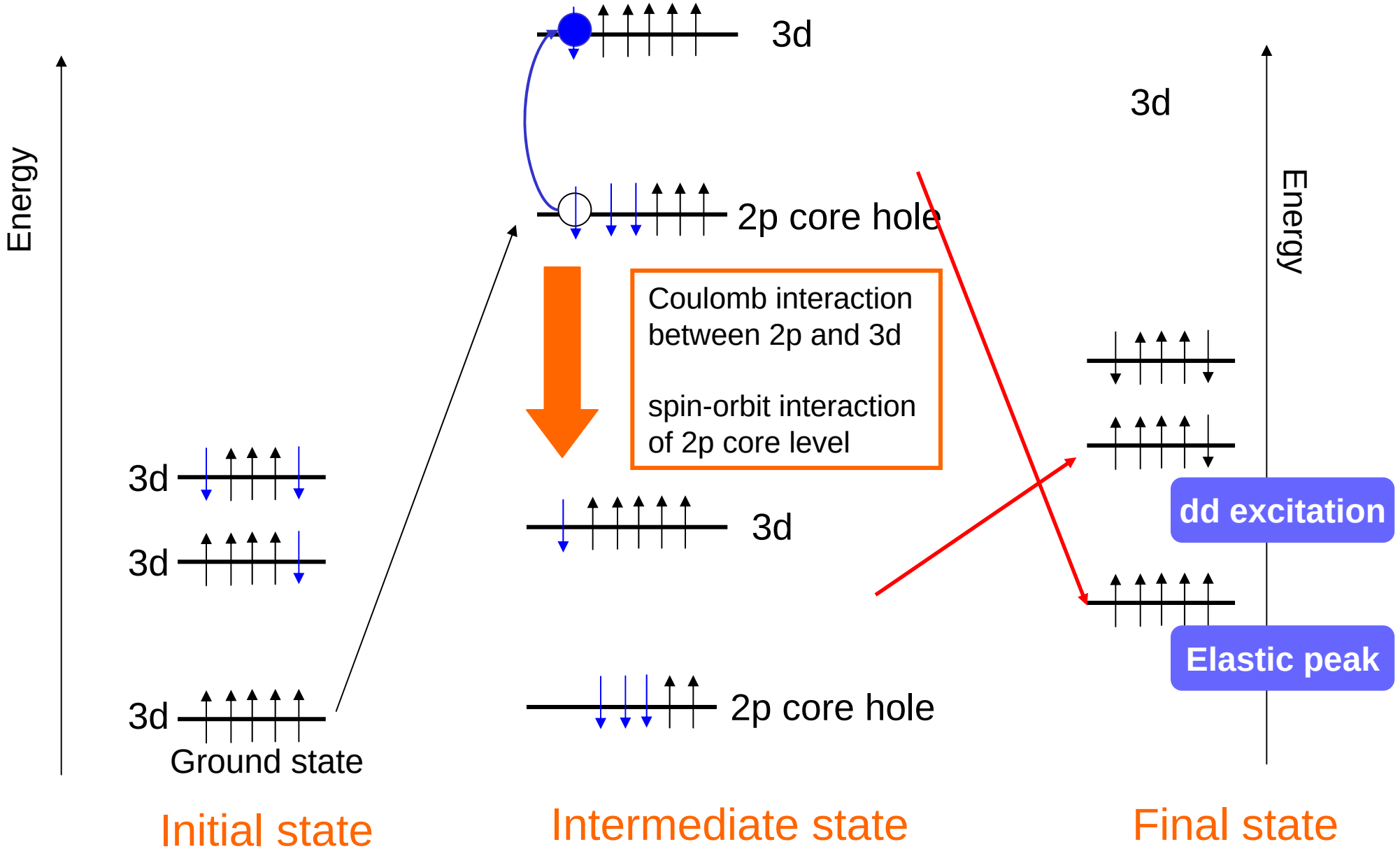

Unraveling hidden *d-d* transitions by resonant inelastic x-ray scattering (RIXS)

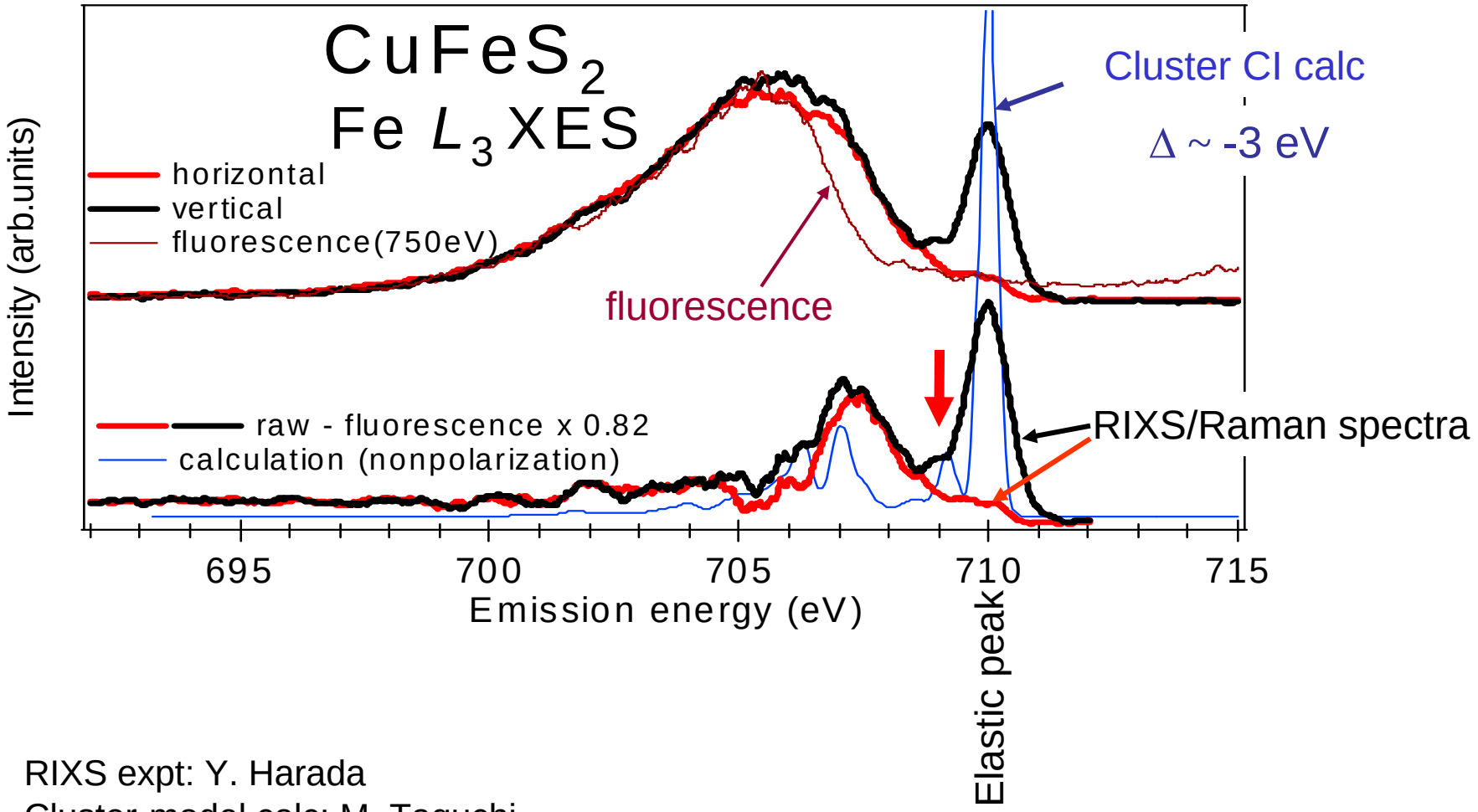

RIXS expt: Y. Harada
Cluster-model calc: M. Taguchi

CI model with full multiplet

Approximations

(I) Central atom: Fe $3d^5$, $3d^6$

Neighboring atom: ligand

Parameters

V(Γ): Hybridization

U_{dd}: On-site Coulomb interaction

U_{dc}: Core-hole potential

Δ: Charge transfer energy

Slater Integrals (Racah parameter) are calculated by Hartree-Fock method and are rescaled by 80%

CI model

$$H = \sum_{\Gamma,\sigma} \varepsilon_{3d}(\Gamma) d^{\dagger}_{\Gamma\sigma} d_{\Gamma\sigma} + \sum_{m,\sigma} \varepsilon_{2p} p^{\dagger}_{m\sigma} p_{m\sigma} + \sum_{\Gamma,\sigma} \varepsilon_{p}(\Gamma) a^{\dagger}_{\Gamma\sigma} a_{\Gamma\sigma}$$

Fe 3d　　Fe 2p　　ligand

$$+ \sum_{\Gamma,\sigma} V(\Gamma)(d^{\dagger}_{\Gamma\sigma} a_{\Gamma\sigma} + a^{\dagger}_{\Gamma\sigma} d_{\Gamma\sigma})$$

Fe3d - ligand charge transfer

$$+ U_{dd} \sum_{(\Gamma,\sigma)\neq(\Gamma',\sigma')} d^{\dagger}_{\Gamma\sigma} d_{\Gamma\sigma} d^{\dagger}_{\Gamma'\sigma'} d_{\Gamma'\sigma'}$$

Fe3d on-site Coulomb interaction

$$- U_{dc}(2p) \sum_{\Gamma,m,\sigma,\sigma'} d^{\dagger}_{\Gamma\sigma} d_{\Gamma\sigma} (1 - p^{\dagger}_{m\sigma'} p_{m\sigma'}) + H_{\text{multiplet}},$$

Fe 2p-3d core-hole potential

Ground state : linear combination of 3 configurations

$$3d^{n} \longleftrightarrow 3d^{n+1}\underline{L} \longleftrightarrow 3d^{n+2}\underline{L}^{2}$$

Experimental results (XES)

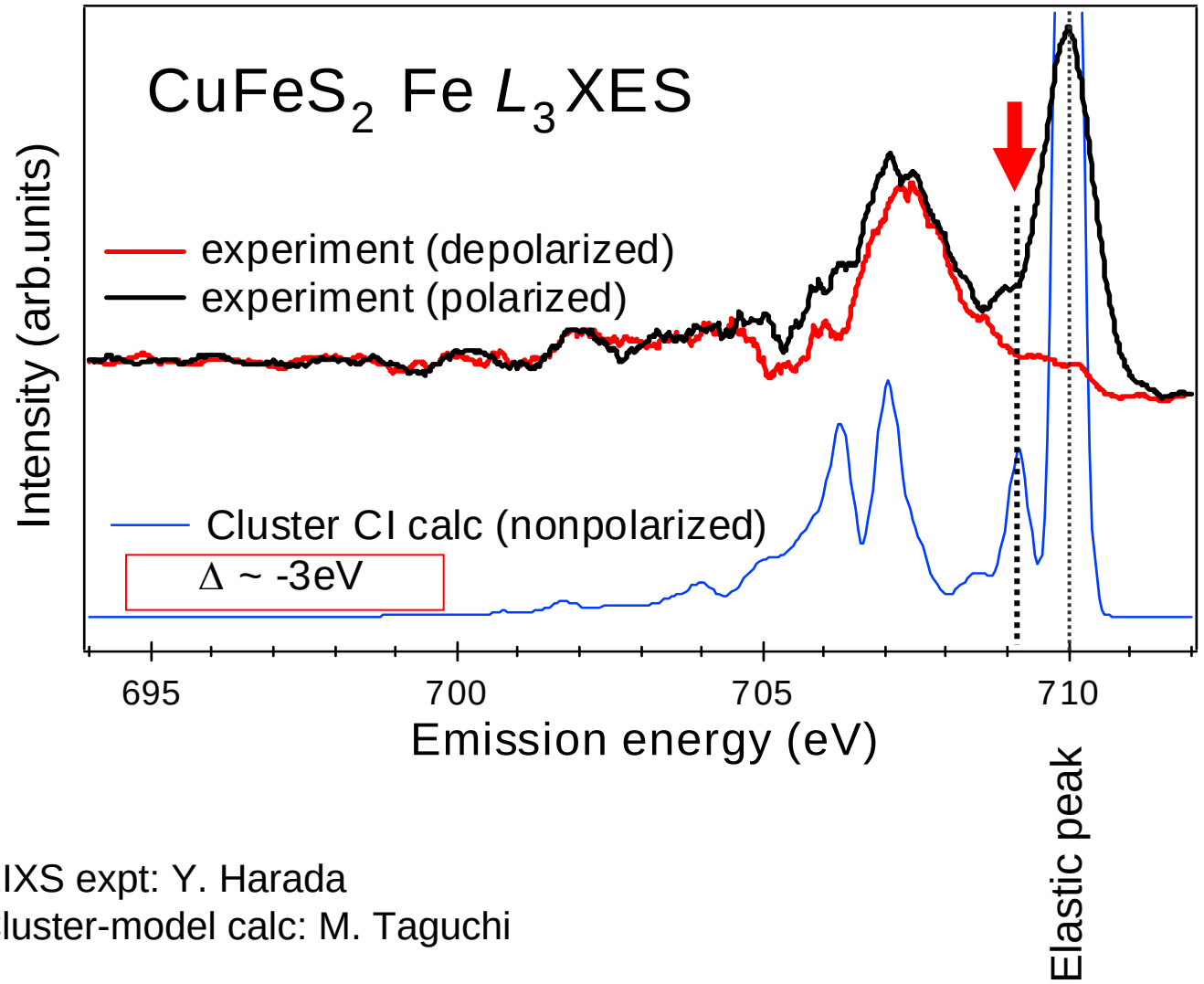

RIXS/Raman spectra
→ *dd* excitation

RIXS expt: Y. Harada
Cluster-model calc: M. Taguchi

Unraveling hidden *d-d* transitions by resonant inelastic x-ray scattering (RIXS)

Ligand-field and CI cluster-model calcs

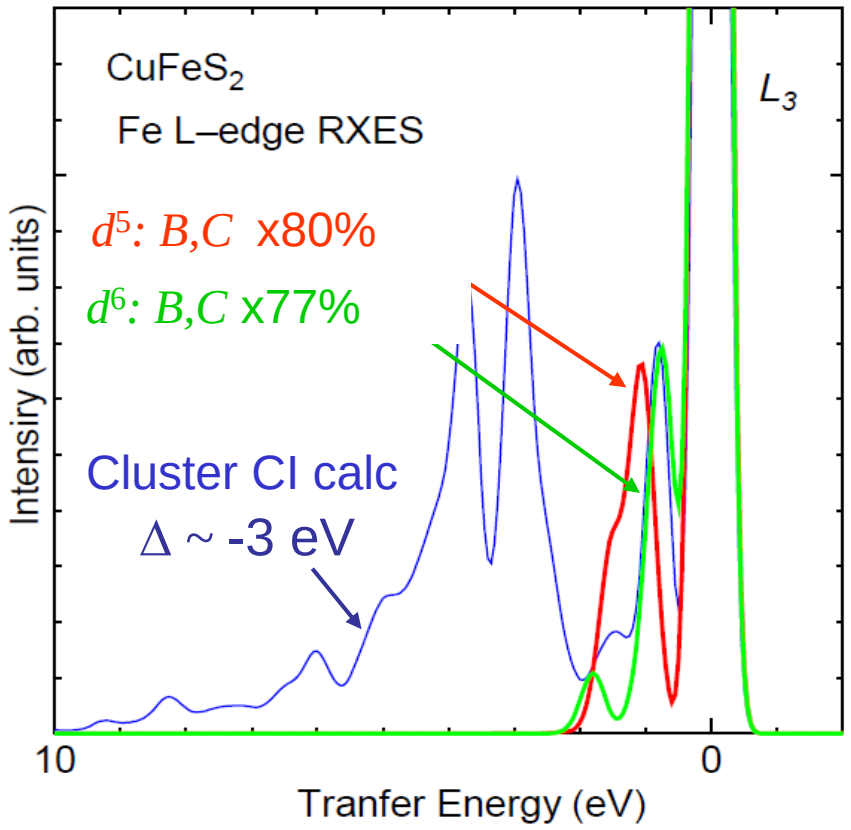

$\Delta < 0$

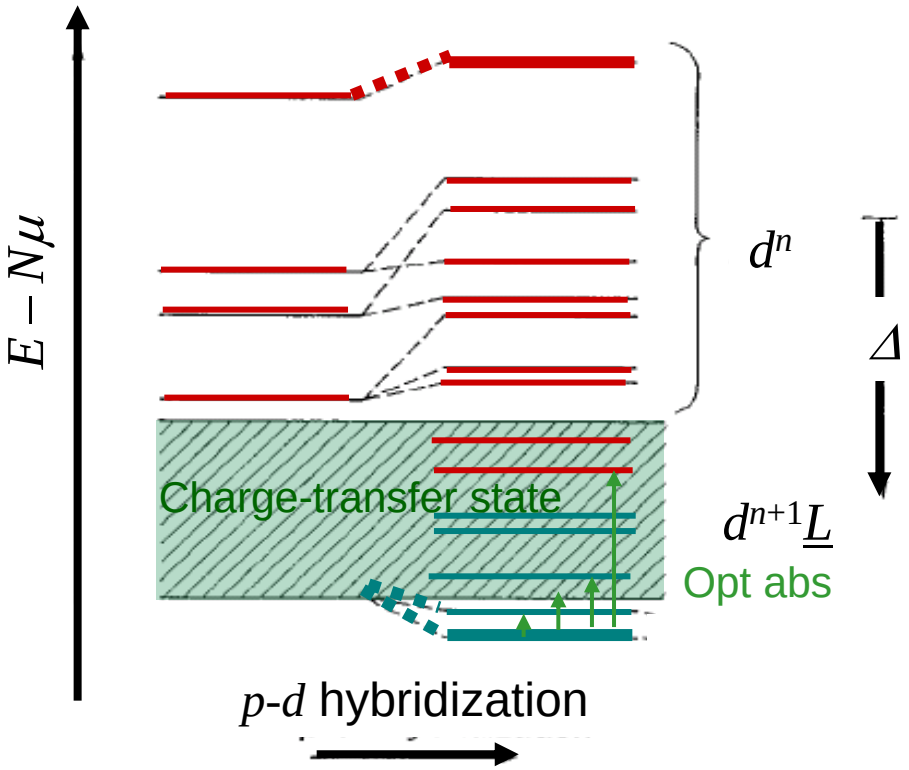

M. Taguchi

Conclusion

- Unusually low energy positions of IR-PL and strong CT absorption in $CuAlS_2$:Fe can be explained by Haldane-Anderson mechanism.
- $CuFeS_2$ is found to be a negative CT energy insulator from PES and RIXS (XES) studies suggesting that this material is a typical “Haldane-Anderson” crystal.